J_ID: APPLAB DOI: 10.1063/1.4997675 Date: 26-October-17 Stage: Page: 1 Total Pages: 6

PROOF COPY [APL17-AR-07249R1] 002745APL

APPLIED PHYSICS LETTERS **111**, 000000 (2017)

NbRe as candidate material for fast single photon detection

M. Caputo, C. Cirillo, and C. Attanasio

CNR-SPIN Salerno and Dipartimento di Fisica "E. R. Caianiello," Università degli Studi di Salerno, Fisciano, Salerno I-84084, Italy

(Received 26 July 2017; accepted 18 October 2017; published online xx xx xxxx)

The suitability of NbRe as a promising material for the design of Superconducting Single Photon Detectors is investigated in order to lower both the minimum detectable photon energy and the recovery time of the devices. Both the low values determined for the quasiparticle relaxation time, τ_E, and its weak temperature dependence are desirable in the design of fast single photon detectors. Both properties can be further improved by coupling NbRe with a ferromagnetic layer, as demonstrated by estimating the characteristic relaxation rates in NbRe/CuNi bilayers. *Published by AIP Publishing.* https://doi.org/10.1063/1.4997675

Superconducting Single-Photon Detectors (SSPDs) represent the state-of-the-art technology for ultrasensitive optical detection[1,2] as well as the new promising key element in the growing field of quantum communication.[3] In the framework of the normal conducting hot-spot (HS) model,[2,4] their operating principle is based on the formation of a normal HS region in a thin current-biased superconducting nanowire due to the absorption of a photon.[4,5] The main advantages of the SSPD technology, compared to the silicon based one,[6] are the cryogenic operating temperature, which substantially reduces noise, and the lower values of the superconducting energy gap, Δ, the minimum energy requested to a photon to create a quasiparticle (qp). The smaller is the value of Δ the higher is the sensitivity and the efficiency of the device,[5] defined as the threshold of the minimum photon energy detectable by the device, $E_{\min}$, and the probability of recording an output signal after a photon hits the detector, respectively. As a first approximation, $E_{\min}$ can be estimated as[4] $E_{\min} \sim \Delta N_0 k_B T_c D d \tau_{th}$, where N_0 is the density of states at the Fermi level, k_B the Boltzmann constant, T_c the superconducting critical temperature, D the electronic diffusivity, d the wire thickness, and τ_{th} the electronic thermalization time. Along with $E_{\min}$, other parameters are relevant for the detection process. First, the maximum HS radius $r_{\max} \propto (E_{ph}/\Delta^2 N_0 d D \tau_{th})^{1/2}(1/N_0\Delta)^{1/3}$ (Refs. 7 and 8) that, in order to achieve good sensitivity, must be comparable to the nanowire width (E_{ph} is the photon energy). This last condition imposes precise constraints to the device geometry, which depend on the E_{ph} as well as on the characteristic material parameters. To reduce $E_{\min}$ and to ensure suitable HS dimensions, the values of Δ, N_0, and D of the superconductor should be as low as possible.[2] It is worth noticing that the expressions reported for $E_{\min}$ and $r_{\max}$, derived in the framework of the normal conducting HS model, are over-simplified even if intuitively understandable. Deeper considerations concerning the possible detection mechanisms in NbRe are reported in the following. Second, the time response of the device, $\tau_{rise/fall}$, designed as a nano-strip of length L and cross section A, depends on the superconducting penetration length, λ, according to $\tau_{rise/fall} \sim L_k = \mu_0 \lambda^2 L A^{-1}$,[1] where L_k is the kinetic inductance. Finally, since the response of the detector is proportional to the bias current, high critical current densities are desirable.[4] Moreover, it was also suggested that[10,11] the performance of a SSPD may strongly depend on the qp relaxation time, τ_E, namely, the time necessary for the system to recover from the photon absorption, through a non-equilibrium process that involves phonons (ph), qp, and Cooper pairs.[12] To date, the material-of-choice in the SSPD field is NbN,[5] a dirty type-II superconductor, characterized by $T_c \sim 16$ K in the bulk form, and small superconducting coherence length, $\xi \approx 3$–4 nm.[13] It follows that even NbN ultrathin films can operate well below T_c at the liquid helium temperature, greatly simplifying the design of the refrigeration systems. Moreover, NbN is characterized by high J_c and fast electronic response.[4,10] However, since NbN has a large gap amplitude, it is efficient in the single-photon detection regime only in a limited frequency range of the InfraRed domain, while the extension of the detection to longer wavelengths, as the ones useful for instance for application in quantum communications over long distances, remains challenging.[14,15] Improvement in the extension of the spectral range can be achieved by further reducing the wire dimensions or by selecting different superconducting materials with smaller values of Δ, N_0, and D.[16] Recently, amorphous superconductors such as MoGe,[17] MoSi,[18] and WSi[9,15] were suggested as alternatives to NbN. In addition to the spectral issue, they are characterized by large values of $r_{\max}$ and, consequently, they present good detection properties also when the dimensions of the wires are larger than those typical for NbN. This last point reduces the concern of non-uniformities or constrictions along the wires, which is more pronounced for narrower nanowires. Unfortunately, these materials present high efficiency at $T < 4.2$ K, with the disadvantage that more complicated refrigeration systems are needed. Here, $Nb_{0.18}Re_{0.82}$ is proposed as a material to fabricate high-performing SSPDs. $Nb_{0.18}Re_{0.82}$ is a noncentrosymmetric superconductor, with a relatively large bulk critical temperature $T_c \sim 9$ K.[19] When deposited in a thin film form, it presents a polycrystalline structure with small crystallites and disorder-dominated transport properties. The small value of $\xi \sim 5$ nm ensures that T_c is above 4.2 K also for films as thin as $d_{NbRe} = 3.5$ nm for which $T_c = 5.3$ K.[20] The relatively high values of J_c[20] should ensure a good detection efficiency. Moreover, preliminary studies performed on $Nb_{0.18}Re_{0.82}$ wide stripes, in the presence of a non-equilibrium state generated by high-bias current,[20] gave low values of τ_E, which are competitive with those estimated for NbN nanowires.[21,22] Finally, since it was largely demonstrated that putting a superconductor in contact with a ferromagnetic (F) layer produces faster relaxation processes,[11,21,23,24] enhances the photoresponse sensitivity,[25,26] and reduces the dark counts,[27,28] the investigation of $Nb_{0.18}Re_{0.82}$/F bilayers was performed, in order to further improve the device performances. $Cu_{0.45}Ni_{0.55}$ was chosen as a F material due to both its tunable low value of the exchange energy,[29] which is not expected to strongly suppress the superconducting order parameter, and its disordered nature,[11,30] which seems to promote the enhancement of some relaxation channels and the temperature independence of τ_E.[31] Indeed, Cu_xNi_{1-x} with similar values of x was already successfully employed for this purpose in Nb and NbN-based hybrid structures,[21,23,25,26] and therefore, a comparison between these hybrids is more straightforward.

$Nb_{0.18}Re_{0.82}$ films and $Nb_{0.18}Re_{0.82}/Cu_{0.45}Ni_{0.55}$ bilayers (hereafter, NbRe and NbRe/CuNi, respectively) were deposited by dc magnetron sputtering on Si(100) substrates in a UHV system at room temperature. The base pressure was $P = 4.4 \times 10^{-8}$ mbar, and the Ar pressure during the deposition was $P_{\rm Ar}^{\rm NbRe} = 3.2 \times 10^{-3}$ mbar and $P_{\rm Ar}^{\rm CuNi} = 8 \times 10^{-3}$ mbar. The thickness of the NbRe film is $d_{\rm NbRe} = 15$ nm, while in the bilayers, $d_{\rm NbRe} = d_{\rm CuNi} = 15$ nm. The samples were patterned by conventional UV lithography into bridges with width $w = 10\,\mu$m and length (between voltage contacts) $L = 100\,\mu$m. The electric transport measurements were performed in a ^{4}He cryostat with a four probe technique using the same procedure described elsewhere.[20,21] The magnetic field, μ_0H, was applied perpendicularly to the plane of the substrate. From the $R(T)$ curves, the values for T_c (at the 50% of the normal state resistance) and the normal state resistivity, ρ_n, were obtained. For the NbRe films, it is $T_c^{\rm NbRe} = 6.77$ K and $\rho_n^{\rm NbRe} = 143\,\mu\Omega \times$cm, while for the NbRe/CuNi bilayers, it is $T_c^{\rm NbRe/CuNi} = 5.86$ K and $\rho_n^{\rm NbRe/CuNi} = 94\,\mu\Omega \times$ cm.

In Fig. 1(a), selection of *I-V* characteristics for different H values at the reduced temperature $t = T/T_c = 0.5$ is shown for a NbRe/CuNi bilayer in the low voltage region. Similar curves were measured on single NbRe bridges.[20] From the *I-V* curves, the critical current I_c was obtained by using a $V_c = 1\,\mu$V criterion. At low magnetic fields, the critical current density, $J_c = I_c/(wd_{\rm NbRe})$, for both samples is $J_c^{\rm NbRe} \sim J_c^{\rm NbRe/CuNi} \sim 5 \times 10^9$ A/m^2, as shown in the inset of Fig. 1.

With the information acquired from the $R(T)$ and V–I curves, it is possible to derive the material parameters relevant for the detection process. Those are compared to the ones reported for a 14.4-nm NbN film,[13] as summarized in Table I. NbRe and NbN have comparable normal state resistivities, since $\rho_n^{NbN} = 117\,\mu\Omega \times$ cm, and diffusivities being $D^{NbRe} = 0.56 \times 10^{-4}$ m^2/s (Ref. 20) and $D^{NbN} = 0.6 \times 10^{-4}$ m^2/s, while the values of T_c (and Δ) are smaller for NbRe, since it is $T_c^{NbN} = 15.25$ K. Indeed, from the values of T_c, the superconducting gaps at $T = 0$ were estimated using the expression $\Delta(0) = (\alpha/2)k_BT_c$,[32] where α is the material coupling constant, $\alpha^{NbRe} = 3.52$ (Ref. 20) and $\alpha^{NbN} = 4.16$,[33] respectively. In this way, it results in $\Delta(0)^{NbRe} = 1.03$ meV and $\Delta(0)^{NbN} = 2.73$ meV. Furthermore, the density of states at the Fermi level was estimated by using the free-electron Einstein's relation $N_0 = 1/(e^2\rho_nD)$,[34] where e is the electron charge; $N_0^{NbRe} = 4.8 \times 10^{47}$ J^{-1}m^{-3} and $N_0^{NbN} = 5.6 \times 10^{47}$ J^{-1}m^{-3}. These differences in T_c, Δ, and N_0 have the important consequences of both reducing $E_{\rm min}$ and increasing the HS dimensions. This last issue concerning r_{max} will be more widely discussed in the following in the framework of the model of Ref. 4. The value of J_c is crucial for achieving high detection efficiency.[2] To estimate the intrinsic value of the ultimate critical current the two materials can support, the value of the depairing current at $T = 0$ was evaluated according to $J_{dp}(0) = (8\pi^2\sqrt{2\pi}/21\zeta(3)e) \times \sqrt{(k_BT_c)^3/\hbar v_F\rho(\rho l)}$,[35] where only microscopical experimental parameters are present and ζ is the Riemann function. From the relation $D = v_Fl/3$, where l is the electronic mean free path, it is possible to derive the values of v_F. For NbRe, it is $l^{NbRe} = 5$ nm (Ref. 36) and therefore $v_F^{NbRe} = 3.36 \times 10^4$ m/s and $J_{dp}(0)^{NbRe} = 2.3 \times 10^{11}$ A/m^2. For NbN, since $l^{NbN} = 0.83$ nm (Ref. 13), it follows $v_F^{NbN} = 2.2 \times 10^5$ m/s and $J_{dp}(0)^{NbN} = 9.3 \times 10^{11}$ A/m^2, a factor of four larger than $J_{dp}(0)^{NbRe}$, which however is an acceptable value for the SSPD performances. Moreover, the penetration depth at $T = 0$ was estimated by using the expression $\lambda(0) = 1.05 \times 10^{-3} \times (\rho_n/T_c)^{1/2}$,[37,38] which results in $\lambda(0)^{NbRe} = 483$ nm and $\lambda(0)^{NbN} = 291$ nm. Larger values of λ determine larger L_k, namely, slower response times. However, this drawback could be circumvented by a proper device AQ3

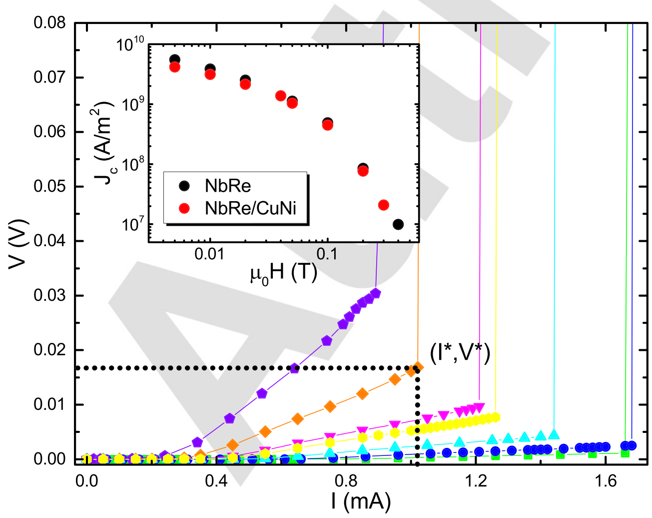

FIG. 1. Low V region of the *I-V* curves for a NbRe/CuNi bilayer at $t = 0.5$ for different values of μ_0H (from right to left $\mu_0H = 0.005$, 0.01, 0.02, 0.04, 0.05, 0.1, and 0.2 T). The current and the voltage where the instability occurs are indicated as I^* and V^*, respectively. Inset: $J_c(\mu_0H)$ dependence at $t = 0.5$ for the NbRe and NbRe/CuNi samples.

TABLE I. Microscopic material parameters for the NbRe bridge and for a NbN one 14.4-nm-thick.[13]

	NbRe	NbN
ρ_n ($\mu\Omega \times$ cm)	143	117
D (10^{-4} m^2/s)	0.56	0.60
T_c (K)	6.77	15.25
$\Delta(0)$ (meV)	1.03	2.73
N_0 (10^{47} J^{-1} m^{-3})	4.8	5.6
$J_{dp}(0)$ (10^{11} A/m^2)	2.3	9.3
$\lambda(0)$ (nm)	483	291

design, for instance, dealing with wider wires reduces $\tau_{rise/fall}$, without affecting the detector efficiency, due to the expected larger HS dimensions. At the same time, the issue of the film uniformity in the nano-patterning processes is expected to be less critical for NbRe-based devices. Finally, information about the spectral sensitivity can now be obtained according to the expression for E_{min} reported above valid in the limit of the normal conducting HS model. By considering for both materials the value measured for thin NbN films, $\tau_{th} = 7$ ps (Ref. 4) since both materials are in the dirty limit, it results in $E_{min}^{NbRe} \sim 0.28$ eV and $E_{min}^{NbN} \sim 1.69$ eV at $t = 0.4$.

Concerning the NbRe and NbRe/CuNi performances in terms of the recovery time, the V–I data at high bias current were analyzed in the framework of the theory of Larkin and Ovchinnikov (LO),[39,40] which provides convenient access to the estimation of the lifetimes of electronic excitations in superconductors as well as in S/F hybrids.[11] As shown in Fig. 1, at small magnetic fields at a certain current value, I^*, a sudden jump takes place. The critical voltage V^* at which the vortex instability occurs is related to the critical vortex velocity, v^*, by the relation $V^* = \mu_0 v^* HL$.[39,40] The jump is replaced by a more continuous transition as $\mu_0 H$ is increased. By defining $\mu_0 H_{max}$ as the maximum field at which the instability is present, it results in, at $t = 0.5$, $\mu_0 H_{max}^{NbRe} = 0.6$ T and $\mu_0 H_{max}^{NbRe/CuNi} = 0.1$ T. In Fig. 2(a), the dependence of v^* as a function of the reduced field, H/H_{max}, is reported for both the NbRe and the NbRe/CuNi bridges at $t = 0.5$. In agreement with the data reported in the literature,[11,21] the S/F bilayer presents higher critical velocities. The qp relaxation time is linked to v^* by the expression $v^* = D^{1/2}[14\zeta(3)]^{1/4}(1-t)^{1/4}/(\pi\tau_E)^{1/2}$.[40] The values of τ_E obtained for the single NbRe bridge at $\mu_0 H_{max}$ are plotted as a function of T in Fig. 2(b), where they are compared with the ones estimated with the same approach for NbN structures of similar dimensions.[21,22] At the saturation, $\tau_E^{NbRe} \approx 200$ ps is about one order of magnitude smaller than the value reported in the literature for NbN. This difference is even more important, if one considers that NbN samples of Refs. 21 and 22 are characterized by smaller dimensions of the bridges.[41] It is worth reminding that the values of τ_E obtained in the framework of the LO theory are different from those estimated from photoresponse experiments as a consequence of different excitation energies.[12] Here, in fact, the non-equilibrium state is produced by the electric field at the center of the vortex instead of being photon-induced by the formation of a current assisted HS. Even if it is not possible to directly connect the two estimations of the relaxation times, it is interesting to note that the scaling between the values extracted within the vortex instability approach and the ones reported in the literature as extracted from optical experiments are the same for NbN and Nb.[10,21] For this reason, it is reasonable to expect that NbRe is characterized by shorter relaxation rates compared to NbN.

The relaxation rates are further reduced for the NbRe/CuNi bilayers. Indeed, from the $\tau_E(T)$ dependence at $\mu_0 H_{max}$ for the NbRe/CuNi dependence reported in Fig. 2(c), it results in $\tau_E^{NbRe/CuNi} \approx 20$ ps, namely, a reduction of τ_E of one order of magnitude in the hybrid compared to the single NbRe bridge. These relaxation times are even faster than the ones of the high performing NbN/CuNi devices of Ref. 21, which are reported for the sake of the clearness in the same figure. This central result of the investigation seems extremely promising for the design of NbRe/F-based photodetectors. It is well known, in fact, that the performance of the devices, in particular, their dead time, crucially depends on the characteristic relaxation rate. Finally, a smooth temperature dependence of $\tau_E(T)$ is shown for the two systems in Fig. 2(d). By fitting the data with a T^{-n} dependence, it results in $n = 0.1$ for both the samples. This value is much smaller than $n = 3$, typical of a dominant e-ph relaxation mechanism.[12] It is reasonable to suppose that these last results have a twofold origin. First, by extending the argument valid for gapless superconductors to proximized F-layers, where Δ is also zero, it results that in these systems the instability appears at larger velocity (and therefore produces a faster relaxation process) due to the fact that the distribution of the normal excitations is less affected by the vortex motion in the gapless system, since they are more uniformly distributed.[39] Second, the disordered nature of both NbRe[20] and CuNi[11,30] produces not only a quasi-constant $\tau_E(T)$ dependence (ensuring a constant response over a wide range of operation temperatures) but also an appreciable reduction of the qp lifetime.[42] Indeed, disorder alters the scattering mechanism, since in dirty films the inelastic processes which lead to energy relaxation may take place only within the vortex core, being the mean free path shorter than the superconducting coherence length. The opposite is true for clean samples. This difference reflects in different dominant relaxation mechanisms: electron-electron recombination in clean samples and e-ph scattering in dirty ones. These interpretations are confirmed by the results observed in

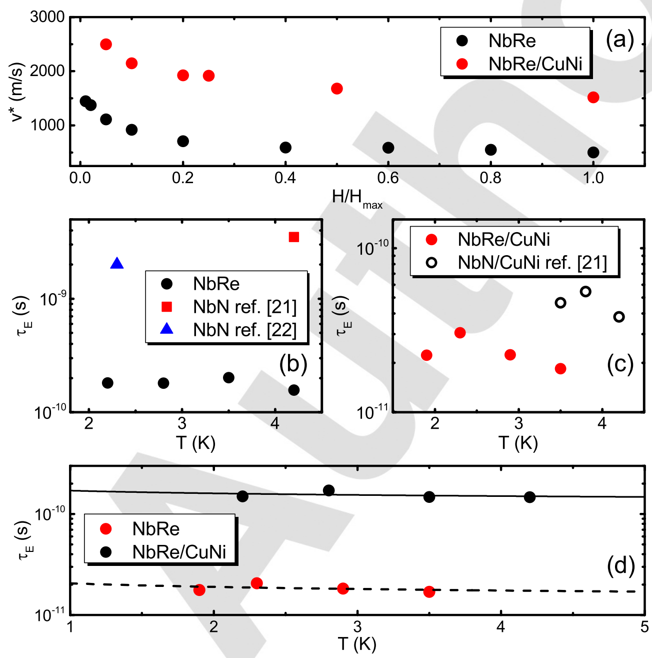

FIG. 2. (a) v^* versus H/H_{max} at $t = 0.5$ for NbRe and NbRe/CuNi bridges. (b) $\tau_E(T)$ dependence at $\mu_0 H_{max}$ for NbRe, compared to NbN structures from Refs. 21 and 22. (c) $\tau_E(T)$ dependence at $\mu_0 H_{max}$ for CuNi-based bilayers, namely, NbRe/CuNi (this work) and NbN/CuNi bilayer (Ref. 21). (d) $\tau_E(T)$ dependence for the NbRe and the NbRe/CuNi bridges at $\mu_0 H_{max}$. The solid and dashed curves are the polynomial fits T^{-n}, with $n = 0.1$ for both the samples.

different S/F hybrids; in particular, the examples of Nb/Py and Nb/CuNi may be useful.[11,31]

From the values of the microscopical parameters reported above for both NbRe and NbN, it is possible to qualitatively simulate also the values of $r_{\max}$ in the framework of the model described in Ref. 4, by using the values of τ_E estimated from the vortex instability analysis at $\mu_0 H_{max}$ and $t = 0.4$, namely, $\tau_E^{NbRe} = 180\,\mathrm{ps}$ and $\tau_E^{NbN} = 3.5\,\mathrm{ns}$.[21] The dependence of $r_{\max}$ on E_{ph} for both the structures, reported in Fig. 3, reveals that r_{max}^{NbRe} is by far larger than r_{max}^{NbN}, which confirms the good potentiality of NbRe for the realization of SSPDs. However, in this analysis, the role of phonons with energies higher than Δ in the evolution of the HS was neglected. While it is possible to estimate the significant energy backflow from phonons to electrons from the ratio $C_{ph}/C_e = 6.4 \times 10^{-3}$, using for the phonon and electron specific heats the values of Ref. 19, the so-called phonon escape time is unknown, since the acoustic matching between the film and the substrate is not available.[10] Before concluding, it is worth commenting also on the model considered to derive the values of E_{min} and $r_{\max}$.[2,4,7] Despite its simplicity, it is still widely used for its capability to describe some important characteristics of SSPDs. Moreover, due to the absence of detailed experimental data on NbRe, it is hard to make valid assumptions on the HS dynamics in this system and consequently to adopt a specific detection model.[2] In addition, too many assumptions on the microscopical parameters should be considered. An accurate analysis of all the models is beyond the scope of this work. However, due to the large values of λ estimated for the NbRe films, it seems reasonable to suppose that vortices may play a role in the detection mechanism and that an increase of E_{min} due to the reduction of the vortex-entry barrier may be observed.[2,9] Experimental investigation of optical devices based on this promising material is highly desirable both to confirm the suitability of NbRe and to shed a light on the detection mechanisms.

In conclusion, electric transport measurements were performed on NbRe and NbRe/CuNi bridges, in order to evaluate their possible application in the field of SSPDs. The results reveal that NbRe-based structures are suitable

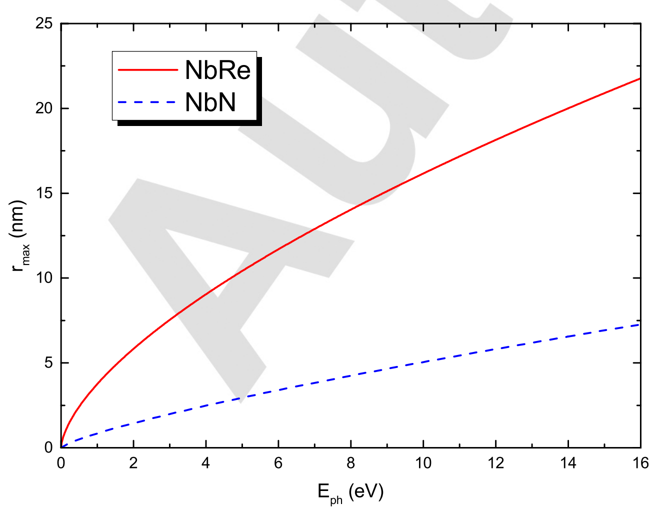

FIG. 3. Numerically calculated radius of the normal HS for NbRe and NbN as a function of E_{ph} at $t = 0.4$.

candidates to successfully design high performing SSPDs. In particular, they could be employed for the detection of single photons of lower energy than NbN, and the estimated HS dimensions suggest that in principle they should require accessible nanowire patterning. Finally, the extremely reduced values estimated for τ_E, in particular, in the case of NbRe/CuNi bilayers, make NbRe-based hybrids suitable candidates for fast operational SSPDs.

The authors wish to thank R. Cristiano and L. Parlato for the valuable discussions and careful reading of the manuscript and Alexey Semenov from DLR Berlin for advices concerning the numerical simulations of the hot-spot dimensions and for providing useful pieces of literature.

[1]C. M. Natarajan, M. G. Tanner, and R. H. Hadfield, Supercond. Sci. Technol. **25**, 063001 (2012).
[2]A. Engel, J. J. Renema, K. Il'in, and A. Semenov, Supercond. Sci. Technol. **28**, 114003 (2015).
[3]K. De Greve, L. Yu, P. L. McMahon, J. S. Pelc, C. M. Natarajan, N. Young Kim, E. Abe, S. Maier, C. Schneider, M. Kamp, S. Höfling, R. H. Hadfield, A. Forchel, M. M. Fejer, and Y. Yamamoto, Nature **491**, 421 (2012).
[4]A. D. Semenov, G. N. Gol'tsman, and A. A. Korneev, Physica C **351**, 349 (2001).
[5]G. N. Gol'tsman, O. Okunev, G. Chulkova, A. Lipatov, A. Semenov, K. Smirnov, B. Voronov, A. Dzardanov, C. Williams, and R. Sobolewski, Appl. Phys. Lett. **79**, 705 (2001).
[6]E. Reigel, S. Dorenbos, V. Zwiller, A. Korneev, G. Chulkova, I. Milostnaya, O. Minaeva, G. Gol'tsman, J. Kitaygorsky, D. Pan, W. Slysz, A. Jukna, and R. Sobolewski, IEEE J. Sel. Top. Quantum Electron. **13**, 934 (2007).
[7]A. Semenov, A. Engel, K. Il'in, G. Gol'tsman, M. Siegel, and H.-W. Hübers, Eur. Phys. J.: Appl. Phys. **21**, 171 (2003).
[8]A. Engel and A. Schilling, J. Appl. Phys. **114**, 214501 (2013).
[9]X. Zhang, A. Engel, Q. Wang, A. Schilling, A. Semenov, M. Sidorova, H. W. Hubers, I. Charaev, K. Ilin, and M. Siegel, Phys. Rev. B **94**, 174509 (2016).
[10]L. Parlato, R. Latempa, G. Peluso, G. P. Pepe, R. Cristiano, and R. Sobolewski, Supercond. Sci. Technol. **18**, 1244 (2005).
[11]C. Attanasio and C. Cirillo, J. Phys.: Condens. Matter **24**, 083201 (2012).
[12]S. B. Kaplan, C. C. Chi, D. N. Langenberg, J. J. Chang, S. Jafarey, and D. J. Scalapino, Phys. Rev. B **14**, 4854 (1976).
[13]A. D. Semenov, B. Gunther, U. Bottger, and H.-W. Hubers, Phys. Rev. B **80**, 054510 (2009).
[14]A. Korneev, P. Kouminov, V. Matvienko, G. Chulkova, K. Smirnov, B. Voronov, G. N. Gol'tsmann, M. Currie, W. Lo, K. Wilsher, J. Zhang, W. Slysz, A. Pearlman, A. Verevkin, and R. Sobolewski, Appl. Phys. Lett. **84**, 5338 (2004).
[15]F. Marsili, V. B. Verma, J. A. Stern, S. Harrington, A. E. Lita, T. Gerrits, I. Vayshenker, B. Baek, M. D. Shaw, R. P. Mirin, and S. W. Nam, Nat. Photonics **7**, 210 (2013).
[16]R. H. Hadfield and G. Johansson, *Superconducting Devices in Quantum Optics* (Springer International Publishing, Switzerland, 2016).
[17]V. B. Verma, A. E. Lita, M. R. Vissers, F. Marsili, D. P. Pappas, R. P. Mirin, and S. W. Nam, Appl. Phys. Lett. **105**, 022602 (2014).
[18]Yu. P. Korneeva, M. Yu. Mikhailov, Yu. P. Pershin, N. N. Manova, A. V. Divochiy, Yu. B. Vakhtomin, A. A. Korneev, K. V. Smirnov, A. G. Sivakov, A. Yu. Devizenko, and G. N. Goltsmann, Supercond. Sci. Technol. **27**, 095012 (2014). AQ4
[19]C. Cirillo, R. Fittipaldi, M. Smidman, G. Carapella, C. Attanasio, A. Vecchione, R. P. Singh, M. R. Lees, G. Balakrishnan, and M. Cuoco, Phys. Rev. B **91**, 134508 (2015).
[20]C. Cirillo, G. Carapella, M. Salvato, R. Arpaia, M. Caputo, and C. Attanasio, Phys. Rev. B **94**, 104512 (2016).
[21]C. Cirillo, V. Pagliarulo, H. Myoren, C. Bonavolontà, L. Parlato, G. P. Pepe, and C. Attanasio, Phys. Rev. B **84**, 054536 (2011).
[22]S. Lin, O. Ayala-Valenzuela, R. D. McDonald, L. N. Bulaevskii, T. G. Holesinger, F. Ronning, N. R. Weisse-Bernstein, T. L. Williamson, A. H. Mueller, M. A. Hoffbauer, M. W. Rabin, and M. J. Graf, Phys. Rev. B **87**, 184507 (2013).

[23]T. Taneda, G. P. Pepe, L. Parlato, A. A. Golubov, and R. Sobolewski, Phys. Rev. B **75**, 174507 (2007).
[24]G. P. Pepe, L. Parlato, N. Marrocco, V. Pagliarulo, G. Peluso, A. Barone, F. Tafuri, U. S. di Uccio, F. Miletto, M. Radovic, D. Pan, and R. Sobolewski, Cryogenics **49**, 660 (2009).
[25]D. Pan, G. P. Pepe, V. Pagliarulo, C. De Lisio, L. Parlato, M. Khafizov, I. Komissarov, and R. Sobolewski, Phys. Rev. B **78**, 174503 (2008).
[26]N. Marrocco, G. P. Pepe, A. Capretti, L. Parlato, V. Pagliarulo, G. Peluso, A. Barone, R. Cristiano, M. Ejrnaes, A. Casaburi, N. Kashiwazaki, T. Taino, H. Myoren, and R. Sobolewski, Appl. Phys. Lett. **97**, 092504 (2010).
[27]R. Cristiano, L. Parlato, U. Nasti, M. Ejrnaes, H. Myoren, T. Taino, R. Sobolewski, and G. P. Pepe, IEEE Trans. Appl. Supercond. **26**, 2200104 (2016).
[28]U. Nasti, L. Parlato, M. Ejrnaes, R. Cristiano, T. Taino, H. Myoren, R. Sobolewski, and G. Pepe, Phys. Rev. B **92**, 014501 (2015).
[29]C. Cirillo, E. A. Ilyina, and C. Attanasio, Supercond. Sci. Technol. **24**, 024017 (2011).
[30]G. Iannone, D. Zola, A. Angrisani Armenio, M. Polichetti, and C. Attanasio, Phys. Rev. B **75**, 064409 (2007). AQ5
[31]E. A. Ilyina, C. Cirillo, and C. Attanasio, Eur. Phys. J. B **83**, 53 (2011).
[32]M. Tinkham, *Introduction to Superconductivity*, 2nd ed. (McGraw Hill, 1996).
[33]Z. Whang, A. Kawakami, Y. Uzawa, and B. Komiyama, J. Appl. Phys. **79**, 7837 (1996).
[34]H. Bartolf, A. Engel, A. Schilling, K. Il'in, M. Siegel, H.-W. Hübers, and A. Semenov, Phys. Rev. B **81**, 024502 (2010).
[35]J. Romijn, T. M. Klapwijk, M. J. Renne, and J. E. Mooij, Phys. Rev. B **26**, 3648 (1982).
[36]J. Chen, L. Jiao, J. L. Zhang, Y. Chen, L. Yang, M. Nicklas, F. Steglich, and H. Q. Yuan, Phys. Rev. B **88**, 144510 (2013).
[37]P. H. Kes and C. C. Tsuei, Phys. Rev. B **28**, 5126 (1983).
[38]A. D. Semenov and G. N. Gol'tsmann, J. Appl. Phys. **87**, 502 (2000).
[39]A. I. Larkin and Yu. N. Ovchinnikov, Sov. Phys. JETP **41**, 960 (1976). AQ6
[40]W. Klein, R. P. Huebener, S. Gauss, and J. Parisi, J. Low Temp. Phys. **61**, 413 (1985).
[41]G. Grimaldi, A. Leo, A. Nigro, S. Pace, A. A. Angrisani, and C. Attanasio, Physica C **468**, 765 (2008).
[42]C. Peroz and C. Villard, Phys. Rev. B **72**, 014515 (2005).